Published in final edited form as:
Cell. 2012 December 7; 151(6): 1229–1242. doi:10.1016/j.cell.2012.10.049.

Early embryonic priming of a miRNA locus predetermines postmitotic neuronal left-right asymmetry in *C. elegans*

Luisa Cochella and **Oliver Hobert**
Department of Biochemistry and Molecular Biophysics, Howard Hughes Medical Institute, Columbia University Medical Center, New York, NY

Abstract

The mechanisms by which functional left/right asymmetry arises in morphologically symmetric nervous systems are poorly understood. Here we provide a mechanistic framework for how functional asymmetry in a postmitotic neuron pair is specified in *C. elegans.* A key feature of this mechanism is a temporally-separated, two-step activation of the *lsy-6* miRNA locus. The *lsy-6* locus is first "primed" by chromatin decompaction in the precursor for the left, but not the right neuron, several divisions before the neurons are born. *lsy-6* expression is then "boosted" to functionally relevant levels several divisions later in the mother of the left neuron, through the activity of a bilaterally expressed transcription factor which can only activate *lsy-6* in the primed neuron. This study shows how cells can become committed early in development to execute a specific fate much later in development and provides a conceptual framework for understanding the generation of neuronal diversity.

INTRODUCTION

Even though the overall anatomy of the nervous system of most animals is bilaterally symmetric, nervous systems display striking left/right asymmetries in the way they sense and process information (Hobert et al., 2002; Sun and Walsh, 2006). How left/right functional asymmetry is superimposed onto a bilaterally symmetric brain is poorly understood, largely because there are few molecular entry points to study this problem. The nematode *C. elegans* represents the only organism to date in which a specific functional left/right asymmetry, in a bilaterally symmetric pair of neurons (the two gustatory neurons ASE left and ASE right), correlates with the left/right asymmetric expression of molecules (putative chemoreceptors) that are required for this functional asymmetry (Ortiz et al., 2009). This system thus provides a means to dissect the regulatory mechanisms that operate during development to impose functional asymmetry onto a bilaterally symmetric structure.

Genetic screens for mutants in which the left/right asymmetric expression of putative chemoreceptors in the ASEL(eft) and ASER(ight) neurons is disrupted, revealed a complex gene regulatory network that acts in postmitotic ASE neurons to control their left/right functional asymmetry (Hobert, 2006). At the core of this network is a bistable feedback loop, composed of two transcription factors, *die-1* (a Zn finger transcription factor) and *cog-1* (a Nkx-type homeobox gene), and a miRNA, *lsy-6,* which directly represses *cog-1*

Correspondence to mlc2155@columbia.edu and or38@columbia.edu.

(Chang et al., 2004; Johnston and Hobert, 2003)(Figure 1). Each of these factors is asymmetrically expressed in the mature ASE neurons: *lsy-6* and *die-1* are expressed in ASEL, and *cog-1* is expressed in ASER (Figure 1). Loss of any of these factors results in the conversion of either ASEL to ASER (*lsy-6* and *die-1* mutants) or of ASER to ASEL (*cog-1* mutants). However, how the asymmetric expression of the three loop components is established remained unanswered.

While the asymmetry of the ASEL and ASER-specific chemoreceptors only manifests itself in the postmitotic ASE neurons, a previous study suggested that differences between the precursors of these two neurons, generated at a very early embryonic stage, were necessary for the postmitotic ASE asymmetry (Poole and Hobert, 2006). The two ASEs derive from lineage branches that diverge at the 4-cell stage. ASEL is a descendant of the ABa blastomere, while ASER derives from ABp (Figure 1). These two blastomeres are initially equipotent but their development diverges due to a Delta/Notch signal from the P2 blastomere to ABp (Priess, 2005). This Delta/Notch signal results, amongst other things, in the repression of two redundant T-box transcription factors, TBX-37 and TBX-38 in the ABp lineage (Good et al., 2004). As a result, TBX-37/38 are exclusively, but transiently expressed in the eight ABa great-granddaughters (Figure 1). The transient expression of TBX-37/38 in the ABa lineage is required for ASEL specification, as in double mutant animals the ASEL neuron converts into another ASER (Poole and Hobert, 2006). However, because TBX-37/38 expression is transient and only observed in the eight ABa great-granddaughters, but not their descendants (Good et al., 2004), it remained unknown how their asymmetric function is relayed to result in postmitotic ASE asymmetry, six cell divisions later. A “memory mark” was postulated to link the function of TBX-37/38 with the asymmetric expression of the loop components (Poole and Hobert, 2006), but the nature of such mark remained unknown.

Despite their asymmetric origin, the two lineages that give rise to the ASEs become symmetric during gastrulation (Figure 1), at least in part due to the action of the proneural transcription factor, HLH-14 (Poole et al., 2011). Several left/right pairs of neuronal precursors develop from these two branches that express *hlh-14*, but only one pair later expresses the Zn finger transcription factor CHE-1 and develops into the ASE neuron pair (Figure 1, Suppl. Figure 1). CHE-1 acts as a terminal selector, binding directly to the promoter of many ASE-expressed genes and activating their expression (Etchberger et al., 2007). CHE-1 is also required to activate expression of the asymmetric loop components *lsy-6, die-1* and *cog-1* (Etchberger et al., 2007; O’Meara et al., 2009; Sarin et al., 2007). Because *che-1* is bilaterally expressed, this suggested that the TBX-37/38-dependent mechanism for inducing asymmetry must integrate with the bilateral activity of CHE-1 to produce asymmetric expression of the loop components.

Here we show that the asymmetry mark that is established by the first embryonic Notch signal is a distinct chromatin state of the *lsy-6* locus itself that affects the responsiveness of the *lsy-6* locus to CHE-1. We identify a *cis*-regulatory element in the *lsy-6* locus that responds to *tbx-37/38* and is necessary for adoption of an open chromatin state in the ASEL lineage, five cell divisions before ASEL is born. This priming of the *lsy-6* locus is necessary for later boosting of expression, mediated by CHE-1 and a separate *cis*-regulatory region. In the absence of priming the *lsy-6* locus adopts a state that is refractory to subsequent boosting by CHE-1 explaining the absence of *lsy-6* expression in ASER despite the presence of CHE-1 in this cell. Our results suggest a mechanism by which an initial morphological asymmetry in the early embryo is transduced through several cell divisions in the form of a transcriptionally primed regulatory locus, to result in asymmetric neuronal function. We suggest that Notch-dependent priming may be a broadly employed strategy for generating asymmetry in the *C. elegans* nervous system.

RESULTS

The miRNA *lsy-6* is the first known asymmetrically expressed gene in the ASE neurons

To understand how asymmetry of the ASEL and ASER neurons is established during development, we systematically analyzed the earliest signs of asymmetric gene expression between the two neurons. We focused on the bistable feedback loop composed of the miRNA *lsy-6* and two transcription factors, *die-1* and *cog-1,* which act genetically upstream of additional gene regulatory factors that we have identified in the past (Sarin et al., 2007). Genetic epistasis analysis previously suggested that *lsy-6* acts upstream of both *die-1* and *cog-1*, but these results were difficult to reconcile with reporter gene-based expression data for these genes available at that time (Johnston et al., 2005). Using fosmid recombineering technology (Tursun et al., 2009), we generated new reporters for the three loop components, based on large (~40kb) genomic clones contained in fosmid vectors with 15–20 Kb of flanking sequence on either side of the gene of interest (Figure 2A). For *die-1* and *cog-1* the reporters produced a fusion protein containing the transcription factor linked to YFP; both reporters fully rescue the mutant phenotypes of the respective genes (Didiano et al., 2010). For the miRNA *lsy-6,* the reporter was made by replacing the 73 bp precursor hairpin with *yfp* (Figure 2A and Suppl. Materials and Methods). The non-recombineered *lsy-6* fosmid also fully rescues the *lsy-6* mutant phenotype (see below).

Expression from the *lsy-6* fosmid reporter is first observed at the end of gastrulation, in the mother cell of the ASEL neuron but not in the mother of ASER. After the ASEL mother cell divides, the *lsy-6* reporter continues to be expressed only in ASEL as the ASEL sister cell dies by apoptosis shortly after. Expression of the *lsy-6* reporter fosmid in ASEL continues throughout embryonic and larval development and into adulthood (Figure 2B, Suppl. Figure 2A). To confirm that endogenous *lsy-6* is indeed asymmetrically expressed from its onset, we used a sensor for endogenous *lsy-6* activity. The sensor consists of a GFP reporter driven by a synthetic promoter which drives bilateral expression shortly after the birth of the ASE neurons, and contains either a control 3′UTR or the *cog-1* 3′UTR which directly binds *lsy-6* (Johnston and Hobert, 2003). Inclusion of the *cog-1* 3′UTR results in marked repression of the reporter, from its onset, only in ASEL (Suppl. Figure 2B). This argues that endogenous *lsy-6* is only present in ASEL shortly after the birth of the ASE neurons, if not earlier, and thus that the fosmid-based reporter accurately reflects *lsy-6* expression.

While *lsy-6* is asymmetrically expressed even in the mothers of the ASE neurons, asymmetric *die-1* and *cog-1* expression becomes apparent more than two hours later, at the threefold stage of embryogenesis, in the postmitotic ASE neurons (Figure 2C and data not shown). The relative timing of asymmetric expression of the loop components (summarized in Figure 2D) and the observation that *lsy-6* acts genetically upstream of *die-1* and *cog-1* (Johnston et al., 2005) suggested that to understand how ASE asymmetry is established, it is necessary to understand how asymmetric expression of *lsy-6* is initiated and how this initiation is linked to the early embryonic asymmetry imposed by the first Notch signal much earlier in embryonic development.

Distinct regulatory elements required for *lsy-6* expression

Previously, we identified a minimal DNA fragment containing the *lsy-6* hairpin and 932 bp of upstream sequence, which was able to rescue the ASEL to ASER conversion of animals carrying a *lsy-6* null allele (Johnston and Hobert, 2003). However, this fragment results in a partially penetrant conversion of ASER into ASEL, suggesting that it also drives ectopic expression of *lsy-6* in ASER (Suppl. Figure 3A). Indeed, a fluorescent reporter which contains these 932 bp of upstream sequence, driving GFP expression, is initially seen in both ASEL and ASER in embryos (Figure 3A,B)(Johnston et al., 2005). The initially bilateral

expression is gradually lost in ASER and by adulthood, expression is largely restricted to ASEL and occasionally, a few other neurons in the head and the tail (Figure 3A,B)(Johnston et al., 2005). The expression pattern produced by this 932 bp element (from now on referred to as "upstream element") is distinct from the expression pattern of the fosmid reporter and the endogenous *lsy-6* activity inferred from the sensor in two ways: 1) it is not restricted to ASEL from the start and 2) it has a later onset of expression (first observed at the twofold stage, considerably after the ASE neurons have been born).

The initially bilateral expression and the ensuing restriction to ASEL of the upstream element can be entirely explained by previously identified regulatory factors and *cis*-regulatory motifs. The upstream element contains a binding site for CHE-1 and both the binding site and *che-1* are required for *lsy-6* expression (Etchberger et al., 2009; Etchberger et al., 2007; Sarin et al., 2007). This initial, *che-1*-dependent bilateral expression of *lsy-6* is then restricted to ASEL through the action of *cog-1,* which acts through two *cis*-regulatory motifs in the upstream element (data not shown). However, since the fosmid-based reporter is expressed earlier and never shows bilateral expression, important *cis*-regulatory information must reside outside of the upstream element.

To identify missing *cis*-regulatory information, we generated transgenes that contained more genomic sequence than the upstream element, but less than the entire fosmid. We found that addition of 1 Kb of sequence immediately downstream of the *lsy-6* hairpin to the reporter containing the upstream element, resulted in the recovery of the earlier onset of expression around the birth of ASEL and the reporter was only expressed in ASEL and never in ASER (Figure 3C and Suppl. Figure 3B). A genomic fragment containing the *lsy-6* hairpin and flanked by the upstream element and the downstream 1 Kb sequence, not only rescued the *lsy-6* null mutant phenotype, but also almost completely eliminated the ectopic induction of ASEL fate in ASER observed with the upstream element alone (Suppl. Figure 3A). The same expression pattern transformation was observed when only 300 bp of downstream sequence (referred to as the "downstream element" from here on), were included in addition to the upstream element (Figure 3C and Suppl. Figure 3B). Moreover, a synthetic reporter in which the downstream element was placed upstream of the upstream element also resulted in an expression pattern similar to that of the fosmid (Figure 3C and Suppl. Figure 3B), demonstrating that the downstream element provides regulatory information at the transcriptional rather than post-transcriptional level. Taken together, these results show that specific and timely expression of the *lsy-6* locus relies on two separate *cis*-regulatory elements, which reside on either side of the miRNA precursor hairpin sequence.

The downstream element directs transcriptional activation early in the lineage that gives rise to ASEL but not ASER

To better understand the contribution of the downstream element to the overall expression pattern of *lsy-6*, we generated a fluorescent reporter in which we took the 300 bp downstream element out of its genomic context and fused it to *gfp* (Figure 4A). The isolated downstream element produced a novel expression pattern that was distinct from that of the upstream element as well as the fosmid reporter (Figure 4A). First, onset of expression is observed very early in the embryo. Lineage analysis by 4D microscopy of embryos carrying the downstream element reporter revealed that expression begins in a few ABa derived blastomeres, only one cell division after the expression of the initial triggers of the ASEL/R asymmetry, *tbx-37/38*. Expression is strong and most consistent in ABalppp, the cell that will give rise to ASEL, and fluorescence persists until the birth of ASEL but fades thereafter. Importantly, the downstream element never drives expression in ABp derived lineages – one of which will give rise to ASER - where the TBX-37/38 proteins are not expressed.

The correlation between expression of the TBX-37/38 proteins and expression driven by the downstream element suggested a causal relationship between the two. Indeed, in *tbx-37/38* double mutant animals, expression of the isolated 300 bp downstream element is completely lost (Figure 4B). Consistent with *tbx-37/38* and the downstream element playing an important role in the expression of *lsy-6*, expression of the *lsy-6::yfp* fosmid reporter is also completely abolished in *tbx-37/38* mutant animals (23/23 mutant embryos have no expression). Conversely, ectopic expression of *tbx-37/38* in ABp descendents - accomplished either by using two distinct heterologous promoters to drive *tbx-38* or by abolishing the Notch signal that represses *tbx-37/38* in ABp - results in ectopic expression of *lsy-6::yfp* fosmid reporter in ASER (Suppl. Figure 4).

The regulation of the downstream element by *tbx-37/38* is possibly direct, since the 300 bp downstream element contains an excellent match to a predicted T-box binding element that is phylogenetically conserved between at least three nematode species. Deletion of this predicted T-box binding sequence caused a delay and reduction of expression of the downstream element (Suppl. Figure 5A,B); since this effect is not as strong as that observed in the *tbx-37/38* mutant embryos, it is possible that either additional cryptic binding sites for TBX-37/38 are present in the downstream element reporter, or that TBX-37/38 act both directly and indirectly via other regulatory factors to initiate *lsy-6* expression.

These observations suggested that the full *lsy-6* locus could perhaps be transcribed in a lineage-specific, *tbx-37/38*-dependent manner 5–6 cell divisions before the birth of the ASE neurons. However, while the early embryonic expression from the downstream element is easily evident when this element is placed upstream of the transcriptional start site (either by itself or upstream of the upstream element as the fourth reporter in Figure 3C), in its downstream location in the context of the full *lsy-6* locus it does not provide easily apparent levels of transcription until close to the birth of ASEL. To test whether the full locus was indeed able to produce low levels of transcript at earlier time points, we performed single molecule fluorescent *in situ* hybridization (smFISH). Since this technique requires more than 40 probes (each ~ 20 nucleotides long) against the RNA of interest in order to obtain a visible signal (Raj et al., 2008), we could not probe directly for the miRNA transcript and therefore rather used probes against the *yfp* transcript encoded by the fosmid-based reporter. We first detected a specific signal around the AB32 stage, in cells from a lineage that also expressed *tbx-38*, suggesting that indeed the *lsy-6* locus is transcribed 5 cell divisions before the onset of fluorescence, in a lineage-specific manner. Initially, the signal consists of a few discrete “dots” (Figure 4C, III–IV) each of which corresponds to a single mRNA molecule (Raj et al., 2008). However, around the time the mother cell of ASEL is born, a cell with a much higher signal can be observed, where individual transcript molecules can no longer be identified (Figure 4C, V–VI). This suggests two phases of expression from the *lsy-6* locus, the first one producing low and the second one high levels of transcription. These two phases of expression from the *lsy-6* locus were independently confirmed by qRT-PCR (Figure 4D).

The results presented so far indicate that the highly specific expression of *lsy-6* exclusively in ASEL requires two *cis*-regulatory modules: the first one located upstream of the *lsy-6* hairpin, controlled by CHE-1; the second one, downstream of the *lsy-6* hairpin, controlled by TBX-37/38. Each of these elements drives expression with different spatio-temporal specificities in isolation but somehow synergize to produce a distinct expression pattern that precisely matches the functional requirements for *lsy-6* (schematically summarized in Figure 4E).

The two regulatory elements act in a prime-and-boost manner to produce the exclusive *lsy-6* expression pattern

To determine the functional relevance of this composite regulatory architecture, we deleted either the 300 bp downstream element, or a smaller 150 bp element contained within the downstream element, from the full genomic locus in the *lsy-6* fosmid reporter. Either deletion abrogated reporter expression at all embryonic and adult stages (Figure 5A and Suppl. Figure 6A). In addition to the later robust reporter expression, deletion of the downstream element also eliminated the early, low-level transcription of the *lsy-6* locus, as measured by smFISH (Suppl. Figure 6B). This loss of expression is not due to loss of the polyA tail since the cleavage and polyadenylation site resides over 400 bp downstream from the deletion (Figure 5A). Not only is the expression of the reporter affected, but the ability of a non-*yfp* tagged, *lsy-6* containing fosmid to rescue the *lsy-6* mutant phenotype is also very strongly affected, if not eliminated, by this deletion (Suppl. Figure 6C). These results seem counterintuitive since the deleted *lsy-6* fosmid constructs contain an intact upstream element, which, in isolation, is sufficient for postmitotic ASEL expression (Figure 3). These findings suggested that while the upstream element can work by itself in an artificial context, its activity in its broader genomic context requires regulatory information provided by the downstream element, apparently to overcome a repressive impact of surrounding genomic sequences.

We considered the following hypothesis for the function of the downstream element. Given that the results described above suggest that *lsy-6* is expressed at low level in the ABa lineage before the birth of ASEL, we reasoned that an early, *tbx-37/38*-dependent transcriptional input into the *lsy-6* downstream element may “prime” the locus in a way that is necessary to permit later “boosting” of expression, mediated by the upstream element and the cognate *che-1* transcription factor, only in ASEL (see final model Figure 7 for visualization). This “priming” event could, for example, result in an open chromatin state of the *lsy-6* locus allowing for access by the later “boosting” factor *che-1.* In the absence of the early activation mediated by the downstream primer element, the *lsy-6* locus would remain closed and thus would lose its competence for being activated by CHE-1 through the upstream booster element.

To test the “prime-and-boost” model, we first manipulated the “priming” phase of the activation (schematically shown in Figure 5B). Specifically, we asked whether restoring early activation of the *lsy-6* locus with the downstream element deleted, using an ectopically provided, non-*tbx-37/38* input into the locus, would also restore later *lsy-6* reporter expression. In order to direct such an ectopic, early input specifically to the *lsy-6* locus we turned to the CHE-1 transcription factor, which we know binds directly to the upstream element of the *lsy-6* locus but is only expressed much later, in the mother of the ASE neurons (Sarin et al., 2009)and Suppl. Figure 1). This experiment asks whether the *lsy-6* locus can be primed, not by providing a priming input through the downstream element, but by doing so through the upstream element. We dosed *che-1* expression in staged embryos at specific time points during embryonic development using a heat-shock inducible promoter and asked whether this could effectively “prime” the *lsy-6::gfp Δ 150* locus and thus restore expression from this reporter ~10 hours later, a time point at which we should be able to detect boosted expression. A pulse of *che-1* during a time window between 100 and 200 minutes after the two-cell stage (with a peak around 4 cell divisions before *che-1* is normally expressed) indeed restored GFP expression, starting approximately 7 hours after the heat shock (Figure 5C and data not shown); note that the delay in GFP expression argues that heat-shock activation does not immediately result in strong *lsy-6* induction but, as our hypothesis predicts, only primes the locus for later boosting). Embryonic heat-shock activation of *che-1* before this window caused early developmental arrest, likely before the ASE neurons are born. Providing CHE-1 after this time window does not result in activation

of the locus and expression of GFP (Figure 5C), showing that indeed the *lsy-6* locus eventually becomes refractory to activation by CHE-1 in the absence of preceding activation, or priming, during early embryonic development.

This experiment provides three conclusions. First, the *lsy-6* locus lacking the downstream element can be reactivated if the locus has been pre-activated (primed) during a precise window during early embryonic development. This effective heat-shock window coincides with the time at which the downstream *cis*-regulatory element was seen to drive transcription, shortly after the expression of *tbx-37/38*. Second, these results demonstrate the existence of a temporal window of opportunity; the normal, late expression of CHE-1 is not able to activate the *lsy-6* locus without efficient priming, but the very same transcription factor is, when ectopically expressed at the right time, sufficient to provide a priming stimulus to the *lsy-6* locus. Third, the observation that CHE-1 is able to substitute for TBX-37/38 in the priming of the *lsy-6* locus suggests that it is not a specific property of the TBX transcription factors that is necessary for priming, but rather it seems that transcriptional activation of the *lsy-6* locus (even by a transcription factor with a completely different DNA binding mode) is sufficient to allow for the later boost of expression, as long as it is provided at the right time point in development. Consistent with the importance of this time window in development, we also found that TBX-37/38 is only able to efficiently activate the *lsy-6* locus when provided at this early embryonic time point and not at later time points (Suppl. Figure 4B).

To further probe the prime-and-boost model, we tested a specific prediction made by this model. Because *tbx-37/38* acts in many different ABa-derived neurons, the *lsy-6* locus should not only be primed in the lineage that gives rise to ASEL, but should also be primed in many other neurons that derive from ABa, and it should not be primed in ABp-derived neurons (schematically shown in Figure 5B). If this were indeed the case, ectopic expression of the *che-1* "booster" late, in postmitotic neurons should be able to activate expression of *lsy-6* only in ABa-, but not ABp-derived neurons. To test this prediction we ectopically expressed CHE-1 using the *gpa-10* promoter (Jansen et al., 1999) in transgenic animals that contain the fosmid-based *lsy-6* reporter. The *gpa-10* promoter drives expression postmitotically, in two pairs of bilaterally symmetric neurons, ADF left and ADF right and ASJ left and ASJ right where, as in the case of the ASEs, the left neuron derives from ABa and the right neuron from ABp. Consistent with our prediction, transgenic animals with *gpa-10* promoter-driven CHE-1 indeed express *lsy-6* in one or two additional neurons only on the left side of the head ganglion; by morphology and position (and the fact that *gpa-10* is not expressed in any other neurons in this region of the head) these are ADFL and ASJL (Figure 5D).

Altogether, these observations support an intersectional "prime-and-boost" model where the *lsy-6* locus is primed specifically in descendants of the ABa lineage, in a manner dependent on the first Notch signal and in particular the transcription factors *tbx-37/38.* This early activation produces a low level of transcription in the lineage that will give rise to ASEL, and prevents the onset of a refractory state, allowing for robust transcription to begin in the mother of ASEL, when CHE-1 (the "booster") is expressed.

Priming of the *lsy-6* locus involves adoption of an active chromatin structure

A key feature of the "prime-and-boost" model for asymmetric *lsy-6* expression is the differential response of the *lsy-6* locus to the bilaterally expressed *che-1* booster. We hypothesized that the differential response of the *lsy-6* locus could be due to distinct, lineage-specific chromatin states. In particular, priming might involve the *tbx-37/38*-dependent establishment of an active chromatin state in the ABa derived lineage but not in the descendants of ABp. To visualize the chromatin status of the *lsy-6* locus with spatio-

temporal resolution we utilized a chromosome-tagging strategy that has been previously employed in *C. elegans* to visualize the localization and the dynamics of the state of compactness of transgenic arrays (Fakhouri et al., 2010; Meister et al., 2010; Yuzyuk et al., 2009). To this end, we generated transgenic arrays containing the *lsy-6* locus labeled with tandem copies of the lac operator (lacO) sequence. When combined with a ubiquitously expressed lac repressor (lacI) fused to GFP, this allows for direct visualization of the transgene (Figure 6A). We integrated the transgenes into the genome, so that each nucleus contains two GFP foci that mark the location and compaction status of the *lsy-6* locus on the transgene. We analyzed three independent, randomly integrated transgenes to minimize the possibility of an effect from the context of the integration site. The development of embryos carrying the labeled transgenes was followed using time-lapsed microscopy, and lineage analysis was used to track the cells of interest.

Paralleling the lineage-specific expression driven by the downstream *cis*-regulatory elements in the *lsy-6* locus, we observed a lineage-specific decompaction of the *lsy-6* locus containing transgene one cell division after TBX-37/38 expression in the ABa great-granddaughters (Figure 6B,C). In a few embryos we can detect decompaction of the *lsy-6* locus one cell division before, at the time when TBX-37/38 are expressed (data not shown), but a lower amount of GFP:LacI at this time point precludes a more accurate analysis at this earlier time. The observed decompaction was more prominent in ABalppp, the blastomere that 5 cell divisions later gives rise to ASEL, as compared to its sister and its cousins (Figure 6B,C). Importantly, decompaction was never observed in ABpraaa, the blastomere that will give rise to ASER, and only very rarely in other ABp derived blastomeres (Figure 6B,C). This lineage-specific decompaction is dependent on the *lsy-6* locus in the transgene as a transgenic array that does not contain the *lsy-6* locus fails to decompact in the ABa lineage (data not shown). A decompacted state has previously been associated with active genes (Dietzel et al., 2004; Tumbar et al., 1999; Yuzyuk et al., 2009) and in our case the spatial and temporal aspects of the decompaction correlate with the expression driven by the 300 bp downstream *cis*-regulatory element and with the appearance of transcripts from the *lsy-6* locus as seen by smFISH.

We have shown so far that the downstream primer element and the activity of *tbx-37/38* are required for early transcription of the locus (Figure 4 and Suppl. Figure 5,6) as well as for the later expression of *lsy-6* (Figure 5A and the loss of *lsy-6* expression in *tbx-37/38* animals described above). We next asked whether the lineage-specific decompaction of the *lsy-6* locus is also caused by TBX-37/38 and requires the downstream element. When we followed the development of *tbx-37/38* mutant animals carrying a labeled *lsy-6* transgene, we found that indeed, the *lsy-6* locus fails to decompact in the ABalppp blastomere (as well as in other ABa derived blastomeres) (Figure 6D and data not shown). Moreover, analysis of embryos carrying a *lsy-6::Δ150* transgene, also showed impaired ability of the locus to decompact in ABalppp (Suppl. Figure 6). Together, these observations suggest that a chromatin rearrangement of the *lsy-6* locus is involved in the early events that prime the locus for subsequent robust expression.

DISCUSSION

The overall logic of establishing directional asymmetry in the *C. elegans* nervous system

We have described here a framework for understanding the overall logic of how functional asymmetry is introduced into the main neurons of the gustatory system of *C. elegans,* ASEL and ASER (Figure 1, Figure 7). A largely bilaterally symmetric differentiation program is induced in the two ASE neurons through the activity of a series of transcription factors that includes the proneural bHLH factor *hlh-14* and the terminal selector *che-1.* Imposed onto this bilaterally symmetric program is an asymmetry program that is triggered by the *lsy-6*

miRNA. This asymmetric component of the ASEL/R differentiation program is a consequence of the distinct lineage histories of the ASEL and ASER neurons, which results in the ASEL neuron bearing a specific “lineage mark”. This lineage mark is generated at the time of the early morphological asymmetry of the 4-cell stage embryo, which puts ABp (the ASER precursor) - but not ABa (the ASEL precursor) - in contact with P2, which sends a Delta/Notch-mediated signal to ABp. This signaling event generates distinct transcriptional outputs in the descendants of the ABa vs. ABp blastomeres from which ASEL and ASER develop, respectively. In ABp descendants, Notch leads to repression of the two T-box transcription factors *tbx-37* and *tbx-38*; thus, in ABa descendants, these factors are available to “prime” a specific locus, *lsy-6,* at the AB16–AB32 stage, long before specific neuronal fates are assigned. The “primed” state is relayed through a specific chromatin configuration at the *lsy-6* locus and persists through the massive reorganization of the embryo in which long- and short-range cellular migrations generate a bilaterally symmetric body plan. As its final consequence, the asymmetrically marked chromatin allows the terminal selector CHE-1, which otherwise controls hundreds of genes in a bilaterally symmetric manner in both ASEL and ASER, to boost *lsy-6* expression only in ASEL, but not ASER.

States of early cellular plasticity provide a window of opportunity to leave a chromatin mark

The timing of the priming of the *lsy-6* locus and the temporal window during which *lsy-6* can be activated to maintain the locus competent for later robust expression are in concordance with a previously described time window during which *C. elegans* embryos are still developmentally plastic (approximately until AB32–AB64)(Yuzyuk et al., 2009). During this time window, developmentally regulated genes become compacted and become less sensitive to activation by ectopically expressed transcription factors. In support of this notion, studies of subnuclear localization of different tissue-specific promoters showed that in the early embryo, arrays are randomly distributed throughout the nucleus, but as development progresses they accumulate at the nuclear periphery in cells where those promoters are not activated (Meister et al., 2010). Taken together, these studies suggest that the *lsy-6* locus may be primed at a time when it is still in a plastic state, through the activity of *tbx-37/38* in the ABa lineage, and that such priming may be necessary to overcome or prevent the onset of a closed or repressed state that would otherwise ensue. The transience of the window for priming of the *lsy-6* locus is also demonstrated by the ability of CHE-1 to substitute for TBX-37/38 if it is provided during that early stage. At later stages, CHE-1 is no longer able to activate *lsy-6* expression without the preceding priming event. It is therefore not the specific nature of the transcription factor that is important to prime the locus, but rather its timing of action.

There appear to be different molecular mechanisms that determine states of regulatory plasticity in the embryo. The studies mentioned above showed that the repressor complex PRC2 restricts plasticity (Yuzyuk et al., 2009). However, the chromatin plasticity at the *lsy-6* locus appears independent of PRC2 since we find that elimination of PRC2 activity does not substitute the need for the priming mechanism; *che-1* is still unable to induce *lsy-6* in PRC2(−) animals in the ASER lineage (unpubl. observation).

In spite of a conceptual similarity, the prime-and-boost mechanism appears distinct from the mechanism of action of pioneer factors, which can bind to compacted nucleosomal DNA, disrupt interactions between nucleosomes and act as placeholders for later joining transcription factors which would otherwise not have access to the locus (Zaret and Carroll, 2011). First, in contrast to pioneer factors, which do not activate gene expression (Fakhouri et al., 2010; Gualdi et al., 1996), the priming event that we describe here involves the transcription of the *lsy-6* locus, albeit at very low levels. Second, priming can be achieved by ectopic, early expression of a transcription factor, CHE-1, that does not normally have

the ability to activate a non-primed locus (because CHE-1 is not sufficient to induce a non-primed *lsy-6* locus in ASER). Third, ectopic expression experiments show that the priming factors TBX-37/38 can only work at an early, but not a late stage in embryogenesis after chromatin compaction. In contrast, pioneering factors should be able to operate independent of the chromatin compaction status of a target locus.

Asymmetric prepatterns and the role of miRNAs in diversifying fates

The priming event mediated by the *tbx-37/38* factors in the ABaXXX cells may constitute an "asymmetry pre-pattern" that is exploited in other cells of the nervous system to generate asymmetry in otherwise bilaterally symmetric neuron pairs. Besides the ASE pair, there are an additional 14 neuron pairs where the left cell derives from ABa, i.e. has been exposed to *tbx-37/38*, while the right cell is derived from ABp. Most of these neuron pairs are sensory neurons for which lateralization, in principle, constitutes an effective way to solve a discrimination problem. The two best-characterized asymmetries in the worm, in the gustatory ASE neuron pair and the olfactory AWC neuron type, are defined by the left/right asymmetric expression of putative chemoreceptors and it is this segregated expression into the left and right neuron that helps the animal to discriminate between distinct chemosensory inputs (Hobert et al., 2002). We predict that a systematic analysis of sensory receptor gene expression may reveal many more asymmetries of this sort and that the ABa vs. ABp-derived neuron pairs are excellent candidates for displaying such asymmetries.

The mode of action of miRNAs predestines these molecules to diversify gene expression programs in related cells. Transcriptional programs that operate in the same manner in two related cells (such as bilaterally symmetric neuron pairs) can be envisioned to be the evolutionarily ancient ground state. The selective recruitment of a miRNA into such a transcriptional program allows for modification of the transcriptional program specifically in only a subset of the initially similar cells. *lsy-6* represents a good example for such recruitment since *lsy-6* exists only in a subset of known nematode species and not in insects or vertebrates. The gain of the *lsy-6* locus may have permitted *C. elegans* to diversify what originally was a bilaterally symmetric ASE neuron pair. The recruitment of *lsy-6* to this regulatory scheme occurred via its ability to respond to a transient "priming" input and secondary "boosting" input that relied on the CHE-1 transcription factor, which also controls the expression of many other genes in the ASE neurons. It will be interesting to see whether other miRNAs similarly diversify the function of the bilateral neuron pairs described above.

A sequential, intersectional mechanism for cell-specific control of gene expression

The prepatterns that were revealed by our analysis in the context of diversifying the fate of two otherwise largely similar neurons across the left/right axis may be a more general strategy for generating diversity of gene expression programs in the nervous system. Neuron type-specific gene expression programs are generally thought to be brought about by intersectional, combinatorial strategies in which neuron type-specific gene batteries are activated by a combination of transcription factors that uniquely overlap in a specific neuron type and directly cooperate to activate target genes. Our results show that such intersectional strategies can be temporally separated. The specificity in *che-1* activating *lsy-6* expression only in ASEL, but not in ASER (where *che-1* is also expressed) is, at least not initially, caused by the presence of another factor that works together with *che-1* specifically in ASEL (as conventional combinatorial models of gene regulation would posit). Rather, it is explained by a temporally segregated, lineage-specific (i.e. ASEL vs. ASER lineage) input into the *lsy-6* locus in the form of an alteration of its chromatin configuration. A key feature of this restriction mechanism is that a chromatin-based prepattern maintains differential, lineage-dependent information in cells that will otherwise adopt the same overall fate. The

prepattern critically refines the activity of later-acting transcription factors by allowing them to trigger downstream regulatory factors in only a subset of related cells.

There are many other neurons in the *C. elegans* nervous system that share many functional and anatomic features and coexpress the same set of transcription factors, but are distinct from one another in, for example, their patterns of synaptic connectivity. These cells often also show distinct lineage histories, and the mechanism to make these superficially similar cell types different from one another, may be based on a similar intersectional, chromatin-based, prime-and-boost mechanism that results in specific gene activation in only a subset of cells. Similar mechanisms may be at work in the vertebrate nervous system where the activity of a transcription factor (or a combination thereof) that is expressed and acts in a pool of neurons may be restricted in a subpool of these through the existence of chromatin-based prepatterns, which may have been selectively induced in the precursors of that particular subpool. Our studies therefore provide a novel conceptual framework for understanding how neuronal diversity is generated.

EXPERIMENTAL PROCEDURES

Strains, transgenes and reporter constructs

A list of all mutants and transgenes used in this study is provided in the Supplemental Material. Generation of the fosmid-based reporters was performed according to the protocol described in (Tursun et al., 2009). Smaller sized reporters were generated by regular cloning into the Fire Kit vector pPD95.75.

Conventional microscopy and 4D Microscopy for lineage analysis

A Zeiss Axioplan 2 equipped with Nomarski and fluorescence optics was used. For all scoring and acquisition of single time point z stacks a short arc mercury lamp was used for fluorophore excitation. For time lapsed z-stacks an LED emitting at 470 nm was used for excitation as it is less toxic to the developing embryos, allowing for acquisition of multiple fluorescent images while preserving viability. Time lapsed images were collected with Time to live software from Caenotec and lineage analysis was aided by SIMI BioCell software (Schnabel et al., 1997). All additional DIC and fluorescent images were collected using Micro-manager (Edelstein et al., 2010).

Visualizing expression and compaction of the *lsy-6* locus

Single-molecule (sm) FISH was done as previously described (Raj et al., 2008) and smFISH and RT-PCR analysis are described in the Supplemental Experimental Procedures. To analyze the compaction state of the *lsy-6* locus, we exploited an approach similar to what has been described by Meister et al., 2010. See Supplemental Experimental Procedures for more details.

Supplementary Material

Refer to Web version on PubMed Central for supplementary material.

Acknowledgments

We thank I. Greenwald, W. Grueber, R. Mann and members of the Hobert lab for helpful discussions and comments on the manuscript. We thank P. Meister, S. Gasser, and S. Mango for advice and reagents, I. Topalidou for help with the smFISH, the CGC for strains, Q. Chen for assistance with microinjections and A. Boyanov for help with obtaining integrated transgenes. L.C. was funded by a postdoctoral fellowship from the Helen Hay Whitney Foundation. This work was funded in part by the National Institutes of Health (R01NS039996-05; R01NS050266-03) and the HHMI.

References

Chang S, Johnston RJ, Frokjaer-Jensen C, Lockery S, Hobert O. MicroRNAs act sequentially and asymmetrically to control chemosensory laterality in the nematode. Nature. 2004; 430:785–789. [PubMed: 15306811]

Didiano D, Cochella L, Tursun B, Hobert O. Neuron-type specific regulation of a 3′UTR through redundant and combinatorially acting *cis*-regulatory elements. RNA. 2010; 16:349–363. [PubMed: 20040592]

Dietzel S, Zolghadr K, Hepperger C, Belmont AS. Differential large-scale chromatin compaction and intranuclear positioning of transcribed versus non-transcribed transgene arrays containing beta-globin regulatory sequences. J Cell Sci. 2004; 117:4603–4614. [PubMed: 15331668]

Edelstein A, Amodaj N, Hoover K, Vale R, Stuurman N. Computer control of microscopes using microManager. Curr Protoc Mol Biol. 2010; Chapter 14(Unit14):20. [PubMed: 20890901]

Etchberger JF, Flowers EB, Poole RJ, Bashllari E, Hobert O. *Cis*-regulatory mechanisms of left/right asymmetric neuron-subtype specification in C. elegans. Development. 2009; 136:147–160. [PubMed: 19060335]

Etchberger JF, Lorch A, Sleumer MC, Zapf R, Jones SJ, Marra MA, Holt RA, Moerman DG, Hobert O. The molecular signature and *cis*-regulatory architecture of a C. elegans gustatory neuron. Genes Dev. 2007; 21:1653–1674. [PubMed: 17606643]

Fakhouri TH, Stevenson J, Chisholm AD, Mango SE. Dynamic chromatin organization during foregut development mediated by the organ selector gene PHA-4/FoxA. PLoS Genet. 2010; 6

Gerstein MB, Lu ZJ, Van Nostrand EL, Cheng C, Arshinoff BI, Liu T, Yip KY, Robilotto R, Rechtsteiner A, Ikegami K, et al. Integrative analysis of the Caenorhabditis elegans genome by the modENCODE project. Science. 2010; 330:1775–1787. [PubMed: 21177976]

Good K, Ciosk R, Nance J, Neves A, Hill RJ, Priess JR. The T-box transcription factors TBX-37 and TBX-38 link GLP-1/Notch signaling to mesoderm induction in C. elegans embryos. Development. 2004; 131:1967–1978. [PubMed: 15056620]

Gualdi R, Bossard P, Zheng M, Hamada Y, Coleman JR, Zaret KS. Hepatic specification of the gut endoderm in vitro: cell signaling and transcriptional control. Genes Dev. 1996; 10:1670–1682. [PubMed: 8682297]

Hobert O. Architecture of a MicroRNA-controlled Gene Regulatory Network That Diversifies Neuronal Cell Fates. Cold Spring Harb Symp Quant Biol. 2006; 71:181–188. [PubMed: 17381295]

Hobert O, Johnston RJ Jr, Chang S. Left-right asymmetry in the nervous system: the Caenorhabditis elegans model. Nat Rev Neurosci. 2002; 3:629–640. [PubMed: 12154364]

Jansen G, Thijssen KL, Werner P, van der Horst M, Hazendonk E, Plasterk RH. The complete family of genes encoding G proteins of Caenorhabditis elegans. Nat Genet. 1999; 21:414–419. [PubMed: 10192394]

Johnston RJ, Hobert O. A microRNA controlling left/right neuronal asymmetry in Caenorhabditis elegans. Nature. 2003; 426:845–849. [PubMed: 14685240]

Johnston RJ Jr, Chang S, Etchberger JF, Ortiz CO, Hobert O. MicroRNAs acting in a double-negative feedback loop to control a neuronal cell fate decision. Proc Natl Acad Sci U S A. 2005; 102:12449–12454. [PubMed: 16099833]

Meister P, Towbin BD, Pike BL, Ponti A, Gasser SM. The spatial dynamics of tissue-specific promoters during C. elegans development. Genes Dev. 2010; 24:766–782. [PubMed: 20395364]

O'Meara MM, Bigelow H, Flibotte S, Etchberger JF, Moerman DG, Hobert O. *Cis*-regulatory Mutations in the Caenorhabditis elegans Homeobox Gene Locus cog-1 Affect Neuronal Development. Genetics. 2009; 181:1679–1686. [PubMed: 19189954]

Ortiz CO, Faumont S, Takayama J, Ahmed HK, Goldsmith AD, Pocock R, McCormick KE, Kunimoto H, Iino Y, Lockery S, et al. Lateralized gustatory behavior of C. elegans is controlled by specific receptor-type guanylyl cyclases. Curr Biol. 2009; 19:996–1004. [PubMed: 19523832]

Poole RJ, Bashllari E, Cochella L, Flowers EB, Hobert O. A Genome-Wide RNAi Screen for Factors Involved in Neuronal Specification in Caenorhabditis elegans. PLoS Genet. 2011; 7:e1002109. [PubMed: 21698137]

Poole RJ, Hobert O. Early embryonic programming of neuronal left/right asymmetry in C. elegans. Curr Biol. 2006; 16:2279–2292. [PubMed: 17141609]

Priess, JR. WormBook, C.e.R. Community. Notch signaling in the C. elegans embryo. WormBook. 2005. http://www.wormbook.org

Raj A, van den Bogaard P, Rifkin SA, van Oudenaarden A, Tyagi S. Imaging individual mRNA molecules using multiple singly labeled probes. Nat Methods. 2008; 5:877–879. [PubMed: 18806792]

Sarin S, O'Meara MM, Flowers EB, Antonio C, Poole RJ, Didiano D, Johnston RJ Jr, Chang S, Narula S, Hobert O. Genetic Screens for Caenorhabditis elegans Mutants Defective in Left/Right Asymmetric Neuronal Fate Specification. Genetics. 2007; 176:2109–2130. [PubMed: 17717195]

Schnabel R, Hutter H, Moerman D, Schnabel H. Assessing normal embryogenesis in Caenorhabditis elegans using a 4D microscope: variability of development and regional specification. Dev Biol. 1997; 184:234–265. [PubMed: 9133433]

Sun T, Walsh CA. Molecular approaches to brain asymmetry and handedness. Nat Rev Neurosci. 2006; 7:655–662. [PubMed: 16858393]

Tumbar T, Sudlow G, Belmont AS. Large-scale chromatin unfolding and remodeling induced by VP16 acidic activation domain. J Cell Biol. 1999; 145:1341–1354. [PubMed: 10385516]

Tursun B, Cochella L, Carrera I, Hobert O. A toolkit and robust pipeline for the generation of fosmid-based reporter genes in C. elegans. PLoS ONE. 2009; 4:e4625. [PubMed: 19259264]

Yuzyuk T, Fakhouri TH, Kiefer J, Mango SE. The polycomb complex protein mes-2/E(z) promotes the transition from developmental plasticity to differentiation in C. elegans embryos. Dev Cell. 2009; 16:699–710. [PubMed: 19460346]

Zaret KS, Carroll JS. Pioneer transcription factors: establishing competence for gene expression. Genes Dev. 2011; 25:2227–2241. [PubMed: 22056668]

Highlights

- The *lsy-6* miRNA is the earliest asymmetrically expressed gene in the ASEL/R neurons
- *lsy-6* is transcriptionally regulated through two distinct *cis*-regulatory elements
- A primer element is necessary for chromatin decompaction only in the ASEL precursor
- The booster element responds to a bilateral activator only in the primed ASEL

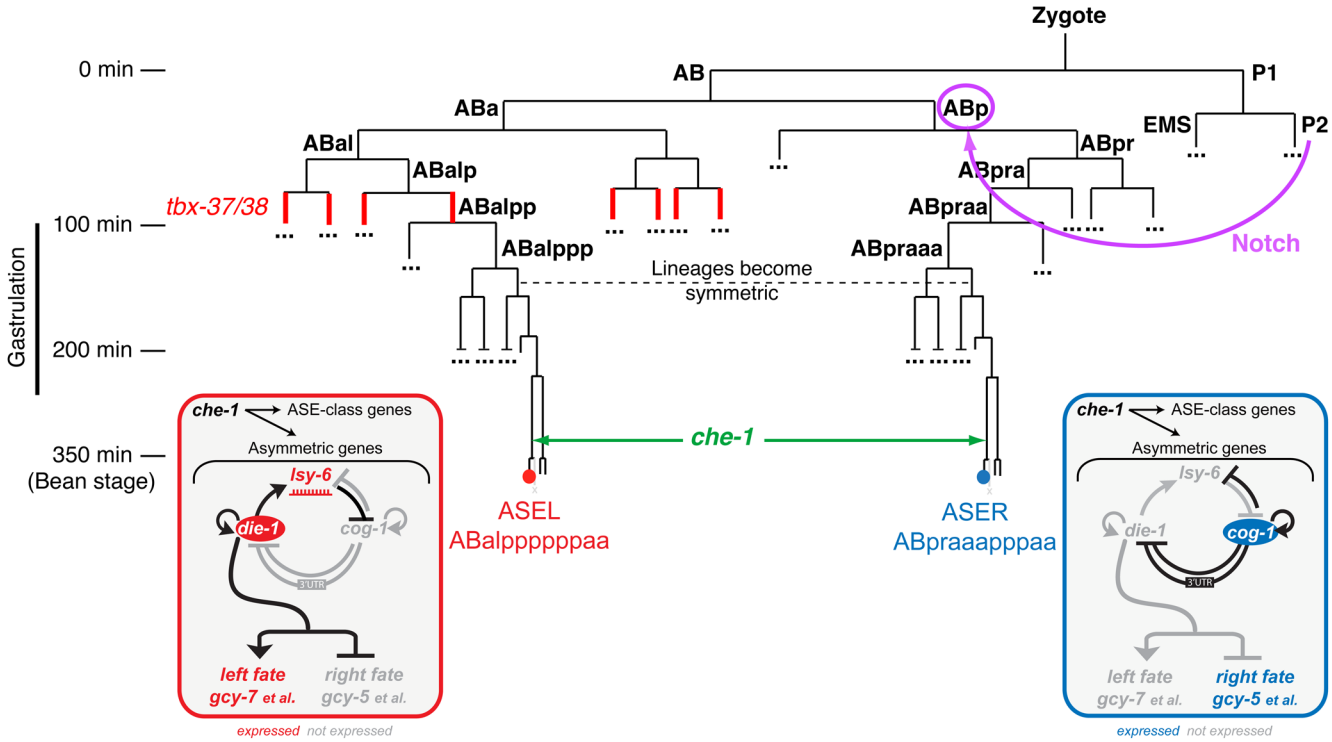

Figure 1. Lineage histories and gene expression of the ASE neurons

Schematic of ASE development. Numbers on the left indicate the approximate timing of the cell divisions. The two boxes show the asymmetric gene expression in the two mature ASEs, with the two alternative configurations of the double-negative loop that result in cell-specific expression of putative guanylate cyclase receptors such as *gcy-7* and *gcy-5.* The onset of CHE-1 expression in the mother of ASE was determined by fosmid reporter expression (Sarin et al., 2009) and by smFISH (Suppl. Figure 1).

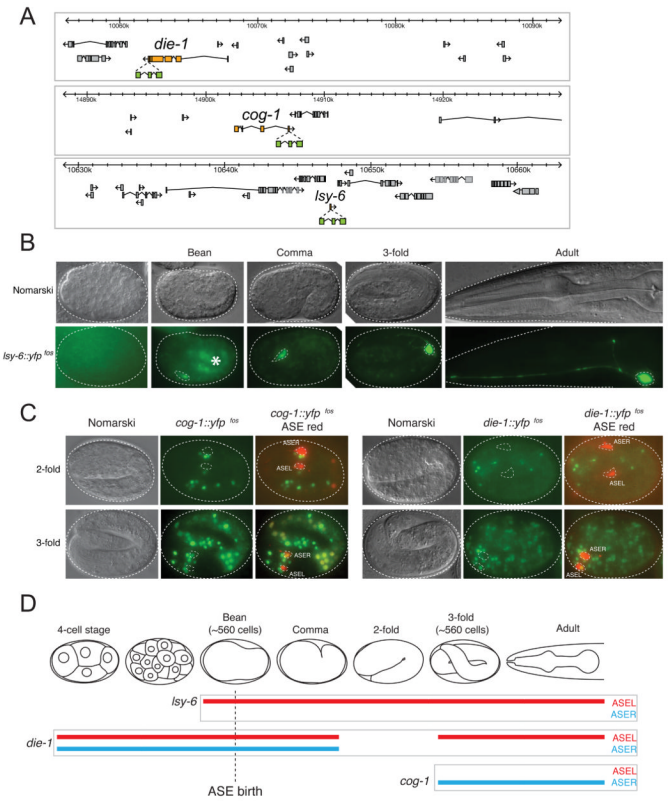

Figure 2. *lsy-6* is the first known asymmetrically expressed component of the loop in the ASE neurons

A. Schematics of fosmid reporter genes.

B. Representative YFP expression in animals carrying the *lsy-6::yfp*^{fosmid} reporter. Expression is first seen around the bean stage, exclusively in ASEL and continues in ASEL until adulthood. Animals and ASEL are outlined. For quantification see Suppl. Figure 2A. * marks autofluorescence from intestinal cells.

C. Expression of fosmid-based *cog-1::yfp* and *die-1::yfp* reporters. Both transcription factors start being expressed in ASE, only at the 3-fold stage, in an asymmetric manner: *cog-1::yfp* in ASER and *die-1::yfp* in ASEL. A bilaterally expressed *che-1*^{prom}*::mCherry* reporter was used to label the two ASEs.

D. Summary of developmental expression of *lsy-6, die-1* and *cog-1* in the ASE neurons.

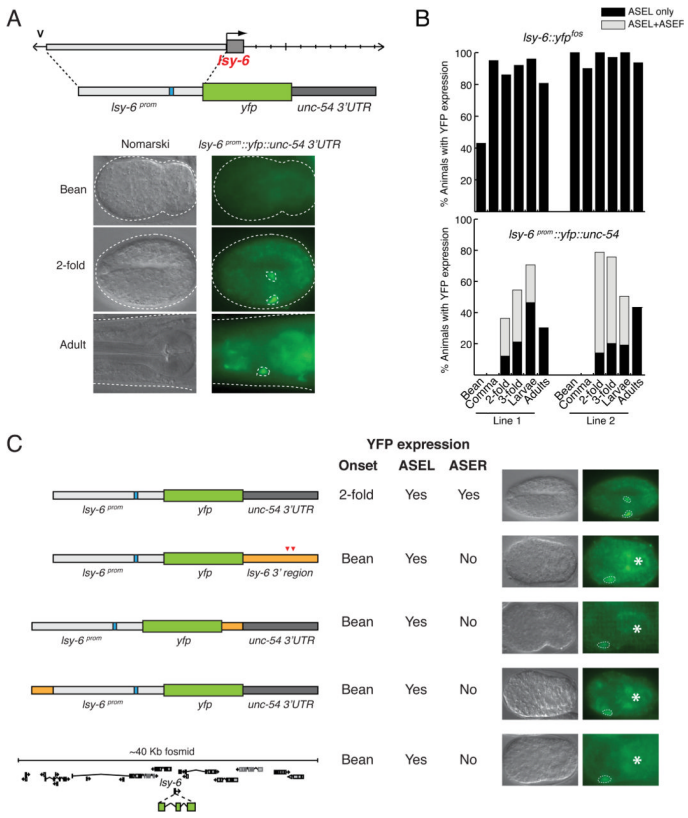

Figure 3. A downstream *cis*-regulatory element is necessary for exclusive *lsy-6* expression in ASEL

A. Schematic of the transcriptional reporter containing the 932 bp upstream element, and representative pictures showing its expression pattern through different stages. Expression begins around the 2-fold stage in both ASE neurons and later gets restricted to ASEL. The blue colored box indicates a functional CHE-1 binding site.

B. Quantification of YFP expression in two independent lines of animals carrying either the *lsy-6::yfp*^{fosmid} or the *lsy-6*^{prom}*::yfp* reporters, throughout different developmental stages. Around 25 animals were scored per time point, per line.

C. A sequence element present downstream of the *lsy-6* hairpin is sufficient to complement the *lsy-6* upstream region to produce an expression pattern most similar to that from the fosmid-based reporter regarding time of onset of expression and exclusivity to ASEL. Red arrowheads show cleavage and polyadenylation sites (Gerstein et al., 2010). The downstream element can be narrowed down to 300 bp (if a 3′UTR containing a functional cleavage and polyadenylation site is included). The 300 bp element also complements expression when placed upstream of the promoter region. * marks autofluorescence from intestinal cells. For quantification see Suppl. Figure 3B.

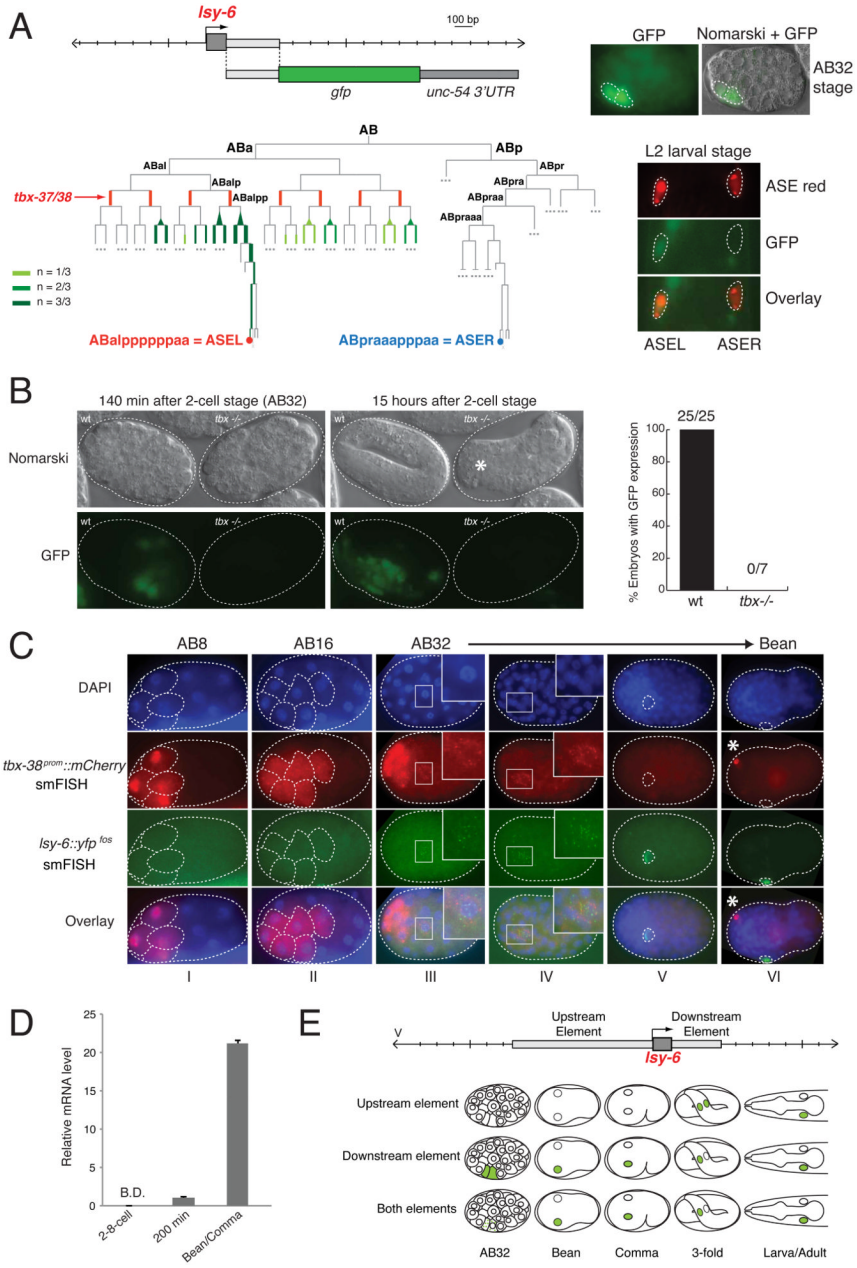

Figure 4. The downstream regulatory element drives expression in the ABa lineage five cell divisions before the birth of ASEL

A. Expression of a transcriptional reporter containing the downstream element driving *gfp* begins early in the embryo and continues into larval stages in a few cells, including ASEL. Lineage analysis of *gfp* expression was carried out on three developing embryos from two independent lines carrying the reporter, using 4D microscopy (Schnabel et al., 1997). Different shades of green represent how many embryos show expression for any given branch. Expression is most consistent in the branch that gives rise to ASEL, while it is never observed in the ABp lineage (or in the mature ASER).

B. Reporter expression driven by the downstream element is lost in *tbx-37/38* double mutants. Representative pictures of a wild-type (either +/+ or +/−) and a double mutant embryo at two stages of development, showing *tbx−/−* animals do not express GFP at any

stage. Embryos are followed from the 2-cell stage until just before hatching. At this stage *tbx−/−* animals are identified due to their characteristic lack of anterior pharynx (*) in addition to their obvious failed morphogenesis. GFP images are analyzed retrospectively to score wild-type and mutant animals. Quantification of this loss of expression is shown to the right (numbers on top of the bars are the number of animals with expression/number of scored animals).

C. Single-molecule FISH against *yfp* and *mCherry* was performed on embryos carrying both the *lsy-6::yfp*^{fosmid} and a *tbx-38*^{prom}*::mCherry* reporter. Embryos were staged according to the number of nuclei and by the number of cells expressing *tbx-38*^{prom}*::mCherry.* See Supplemental Experimental Procedures for more detail on the procedure. Transcription from the *lsy-6::yfp*^{fosmid} is first seen around the AB32 stage (III), consistent with the timing of expression of the downstream transcriptional reporter (**A**) in cells that belong to the ABa lineage and thus also express *tbx-38*. Transcription off of *tbx-38*^{prom} begins in the 4 ABa granddaughters (I), when the transcript is still in the nucleus, and reaches its highest level in the 8 great granddaughters (II), consistent with antibody staining (Good et al., 2004). However, some mCherry mRNA from this promoter fusion seems to persist longer than endogenous TBX-38 and we can use this to trace the ABa lineage. Asterisk at the bean stage (VI) marks expression from a co-injection marker, *ttx-3*^{prom}*::mCherry*. The outlines of the embryos are indicated with dashed white lines as well as the outlines of the *tbx-38*^{prom}*::mCherry* expressing cells in I and II and the outlines of ASEL (VI) and what is very likely its mother (V). Insets in III and IV show close up views of the boxed areas. We furthermore note that smFISH that measures transcription from the endogenous *che-1* locus reveals transcription at around the same time as a *che-1* fosmid reporter transgene (Suppl. Figure 1), demonstrating that smFISH does not simply pick up spurious transcription.

D. Semi-quantitative, real-time RT-PCR analysis confirms the early, low-level transcription of the *lsy-6* locus several cell divisions before the birth of the ASE neurons (200 minutes post 2-cell stage time point; see Supplemental Experimental Procedures).

E. Summary of the expression patterns of each of the two isolated *cis*-regulatory elements and the outcome of both acting together.

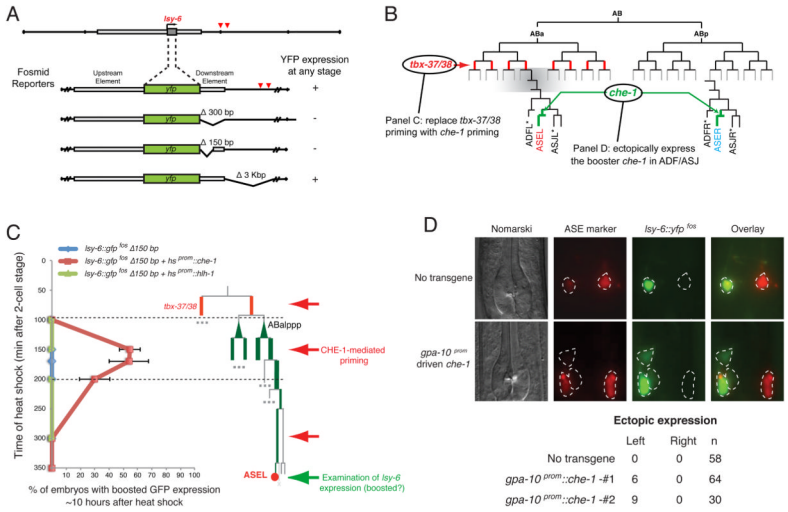

Figure 5. Early activation, or "priming", of the *lsy-6* locus is necessary to maintain the locus competent for subsequent activation

A. Schematic of the deletions generated in the *lsy-6::yfp*^{fosmid} reporter. Deletion of the downstream *cis*-regulatory element abolishes expression from the genomic locus. The red arrowheads show two functional cleavage and polyadenylation sites (Gerstein et al., 2010). A 3 Kb deletion that leaves the 150 bp element intact does not affect expression (for quantification see Suppl. Figure 6A; the 3′ downstream gene likely provides a cleavage and polyadenylation site in this construct).

B. Schematic representation of the key regulators of *lsy-6* expression and the experimental approach taken in panels C and D. *tbx-37/38* are required for the downstream element-mediated, low level expression of *lsy-6* (indicated with a grey box), *che-1* is required for boosting *lsy-6* expression in the ASEL mother cell. In panel C, the transient *tbx-37/38* input into the locus is eliminated by removal of the downstream element and substituted by a transient *che-1* input. In panel D, the activity of the *che-1* gene is broadened to other neurons in which the *lsy-6* locus may also have been primed by *tbx-37/38*.

C. Artificial activation of the *lsy-6::gfp*^{fos} *Δ150* through ectopic, heat-shock induced, expression of CHE-1 (schematized by the red arrows) restores GFP expression from this reporter (measured at the time the ASEs are born, green arrow), only when provided during a specific time window. This window coincides with the time of expression of the downstream element and the onset of transcription from the fosmid reporter seen by smFISH (Figure 4A,C). GFP expression is not only observed in ASEL but also in a few additional cells, likely including ASER. Heat-shock treatment of embryos without the heat shock inducible CHE-1 or expressing the unrelated TF HLH-1, do not result in GFP expression. N is 15–43 embryos for each time point shown.

D. The *lsy-6* locus is primed in multiple descendants of the ABa lineage. Ectopic expression of CHE-1 under the *gpa-10* promoter (active in the ADFL/R and ASJL/R neurons) causes expression of the *lsy-6::yfp*^{fosmid} in two additional cells, only on the left side of the head, that based on position and morphology are identified as ADFL and ASJL. These two cells are closely related to ASEL by lineage and their shared precursor shows expression of the *lsy-6* downstream element. Although the *gpa-10* promoter also drives expression of CHE-1 in ADFR and ASJR, expression of *lsy-6::yfp*^{fosmid} is never observed in these cells.

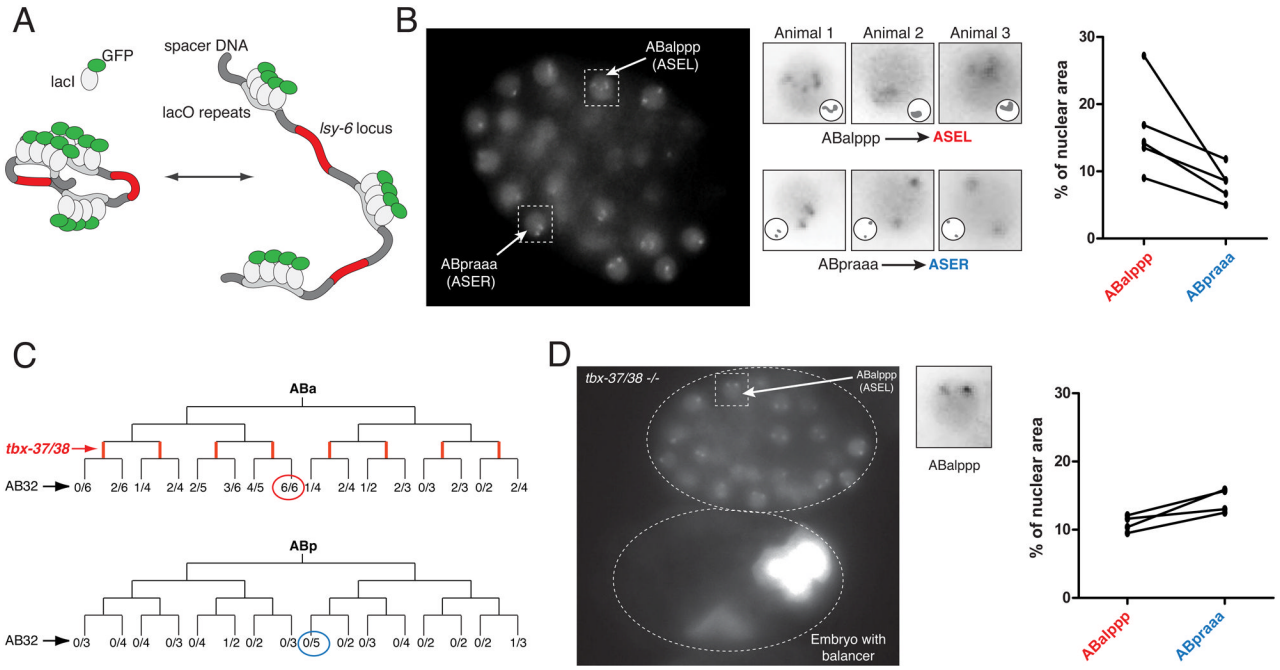

Figure 6. Priming of the *lsy-6* locus involves the establishment of an active chromatin structure, in a *tbx-37/38*-dependent manner

A. Schematic of the array used for visualization of the *lsy-6* locus. A fragment of the *lsy-6* locus containing 932 bp upstream and 1 Kb downstream was co-injected together with binding platforms containing 256 lacO repeats and bacterial genomic DNA as spacer and to increase sequence complexity. These arrays can be visualized through the binding of a GFP::LacI fusion protein.

B. Representative images from one of the 4D series of images of embryos carrying chromosomally integrated, lacO labeled *lsy-6* locus. The precursors of ASEL and ASER at the AB32 stage (the cell division right after *tbx-37/38* expression) are boxed. The image is a maximum-intensity projection of the planes that span the nuclei of interest. Close-up, color inverted, images of their nuclei are shown to the right (Animal 1), as well as the respective nuclei from two additional embryos carrying the labeled locus. Manual traces of areas of GFP accumulation are shown in the insets. As a measure of compaction/decompaction, we assessed the area of the nucleus that has GFP intensity above background, from maximum-intensity projections obtained for both relevant nuclei. A 2-fold larger area is occupied by the *lsy-6* transgene in ABalppp as compared to ABpraaa (P=0.02). N=6. Embryos from three independent integration events were analyzed.

C. Quantification of the number of embryos with a de-compacted *lsy-6* locus in all ABa and ABp derived branches at the AB32 stage. These numbers were obtained from 8 embryos, each carrying one of three independent *lsy-6/lacO* integrated transgenes and are expressed as number of decompacted nuclei/number of nuclei scored for each branch.

D. Decompaction of the *lsy-6* locus fails to occur in *tbx-37/38* mutant embryos. A representative frame from 4D series of images of embryos from *tbx-37/38* heterozygous mothers, carrying the lacI/lacO arrays is shown. The two mutant alleles are present over a balancer marked with an embryonically expressed *gfp,* such that homozygous mutant embryos can be easily identified by the absence of the balancer. The ASEL precursor for this embryo is boxed and a close up is shown. A comparison of the nuclear areas occupied by the *lsy-6* transgene in the two ASE precursors (as calculated in panel B) is shown in the plot to the right.

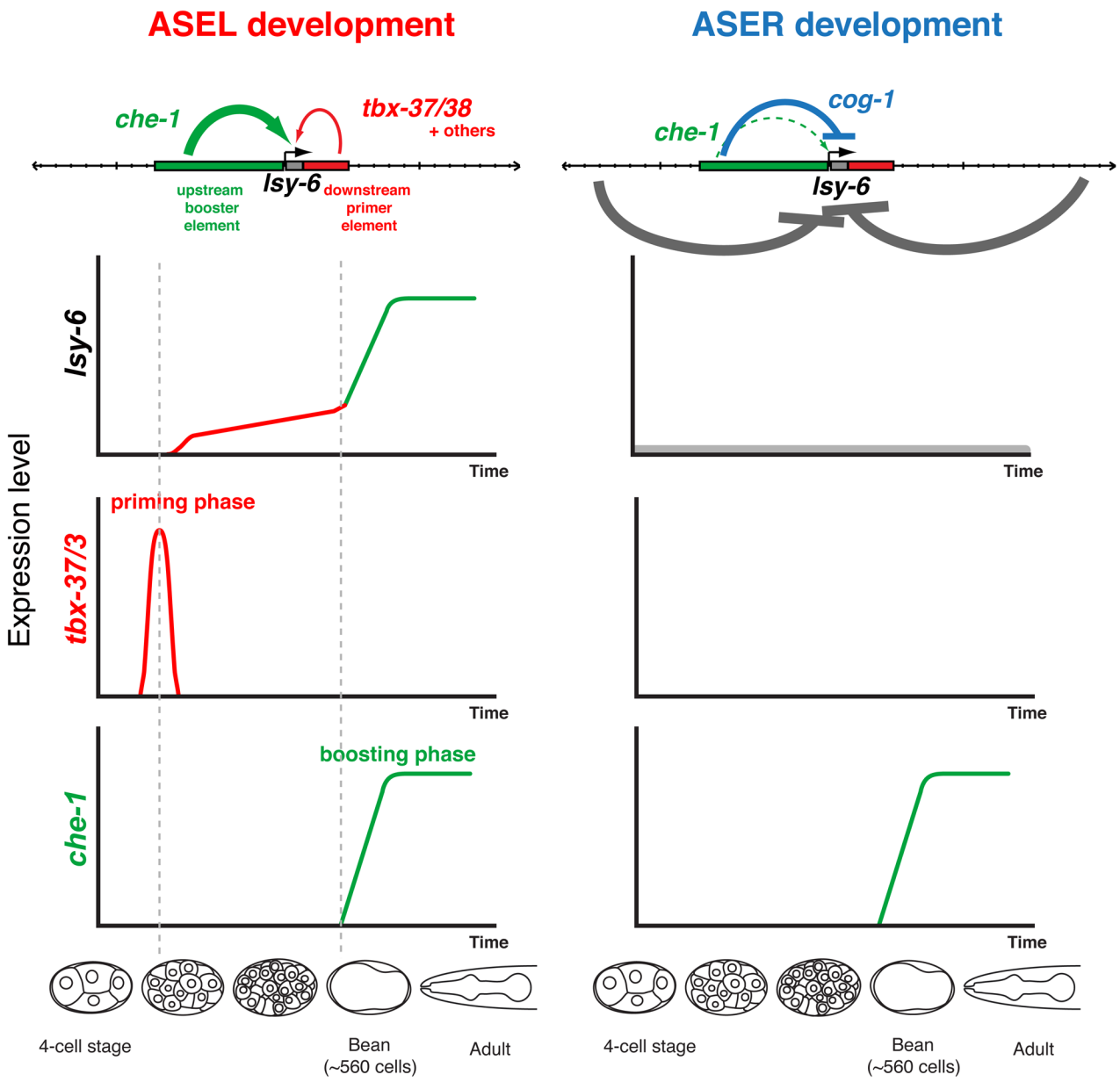

Figure 7. Summary of the mechanistic framework for the establishment of ASE lateral asymmetry

Schematics of the two *cis*-regulatory elements in the *lsy-6* locus are shown, as well as the relevant *trans*-acting factors for its expression and their timing of action. The function of the transient expression of TBX-37/38 exclusively in the ABa lineage is necessary to prime the *lsy-6* locus 6 cell divisions before ASEL is born, producing low levels of transcription from this locus, and establishing a lineage-specific, open chromatin conformation. Priming of *lsy-6* allows for a boost of expression through the action of CHE-1, which is present in both ASE neurons, producing high levels of *lsy-6* only in the postmitotic ASEL. In ASER, absence of *tbx-37/-38* leaves *lsy-6* in a refractory state that does not respond to the presence of CHE-1. Additional repression of *lsy-6* by COG-1 in ASER ensures that the miRNA will not be produced in this neuron (unpubl. data). Once the *lsy-6* asymmetry is established, the rest of the asymmetric gene expression program in the ASEs is defined.